28p

NATIONAL AERONAUTICS AND SPACE ADMINISTRATION

PROPOSED JOURNAL ARTICLE

RECENT ADVANCES CONCERNING THE TRANSPORT PROPERTIES OF DILUTE GASES

by Richard S. Brokaw

Lewis Research Center
Cleveland, Ohio

Prepared for

International Journal of Engineering Sciences

64-43

RECENT ADVANCES CONCERNING THE TRANSPORT PROPERTIES OF DILUTE GASES

Richard S. Brokaw

Lewis Research Center
National Aeronautics and Space Administration
Cleveland, Ohio

ABSTRACT

29397

Some theoretical and experimental developments of the last decade are discussed with emphasis on techniques that can be used to calculate viscosity, thermal conductivity, and diffusion coefficients assuming appropriate interatomic or intermolecular force laws. Three main topics are considered: First, intermolecular potential energy functions for which collision integrals are now available; second, heat conduction in chemically reacting gases; and finally, a closely related topic, the heat conductivity of polyatomic gases.

Author

INTRODUCTION

This paper considers theoretical and experimental developments concerning the transport properties since about 1954; in other words, since the publication of "Molecular Theory of Gases and Liquids" by Hirschfelder, Curtiss, and Bird[1], which effectively summarizes most prior work. Furthermore, the discussion is limited to techniques that have engineering usefulness - techniques that can be used to actually compute transport properties algebraically.

Thus, three main topics are discussed: First, the collision integrals, basic to transport property calculations, that are now available for a wide variety of intermolecular force laws; secondly, heat conduction in chemically reacting gases followed; finally, by consideration of a closely related subject, the thermal conductivity of polyatomic gases.

In general this review will make reference to the literature rather than presenting computational methods as such. Equations will be avoided except insofar as they serve to illustrate the behavior of various properties. Thus,

in order to carry out any actual calculations, the reader must consult the literature.

POTENTIAL ENERGY FUNCTIONS AND THE COLLISION INTEGRALS

The rigorous Chapman-Enskog theory yields the following expressions for the transport properties of dilute monatomic gases[2]:

Viscosity

$$\eta = \frac{5}{16}\left(\frac{\sqrt{\pi mkT}}{\pi\sigma^2\Omega(2,2)^*}\right) \tag{1}$$

Thermal conductivity

$$\lambda = \frac{25}{32}\left(\frac{\sqrt{\pi mkT}}{\pi\sigma^2\Omega(2,2)^*}\right)\left(\frac{c_v}{m}\right) \tag{2}$$

Self-diffusion coefficient

$$D = \frac{3}{8}\left(\frac{\sqrt{\pi mkT}}{\pi\sigma^2\Omega(1,1)^*}\right)\left(\frac{1}{\rho}\right) \tag{3}$$

These formulas involve quantities such as the atomic mass m, the Boltzmann constant k, the temperature T, the heat capacity c_v $(= \frac{3}{2}k)$, and the density ρ, which are well known. However, the formulas also contain cross sections, or more properly collision integrals $\sigma^2\Omega(2,2)^*$ and $\sigma^2\Omega(1,1)^*$, and to compute these the intermolecular force law must be known.

For a spherically symmetric potential, which may be written in a dimensionless form as

$$\frac{\varphi(r)}{\epsilon} = \varphi^* = f\left(\frac{r}{\sigma}\right) = f(r^*) \tag{4}$$

the collision integrals are obtained by a triple integration. (Here ϵ is an energy and σ is a distance characteristic of the potential.) First it is necessary to compute the angle of deflection:

$$\chi(g^*,b^*) = \pi - 2b^* \int_{r_m^*}^{\infty} \frac{dr^*/r^{*2}}{\sqrt{1 - \frac{b^{*2}}{r^{*2}} - \frac{\varphi^*}{g^{*2}}}} \tag{5}$$

where $b^* = b/\sigma$ is the reduced impact parameter. (The impact parameter b is the distance of closest approach in the absence of the potential φ.) Further, $r_m^* = r_m/\sigma$, where r_m is the distance of closest approach in the presence of the potential, and $g^{*2} = \frac{1}{4} mg^2/\epsilon$ is the reduced relative kinetic energy (g is the initial relative speed of the colliding molecules).

Once the angle of deflection has been obtained as a function of g^* and b^*, a velocity-dependent cross section is computed:

$$Q^{(l)*}(g)^* = \frac{2}{\left[1 - \frac{1}{2}\frac{1 + (-1)^l}{1 + l}\right]} \int_0^{\infty} (1 - \cos^l \chi) b^* db^* \tag{6}$$

Finally, the $Q^{(l)*}$ are averaged over all velocities, with an appropriate weighting factor:

$$\Omega^{(l,s)*}(T^*) = \frac{2}{(s+1)!T^{*s+2}} \int_0^{\infty} e^{-g^{*2}/T^*} g^{*2s+3} Q^{(l)*} dg^* \tag{7}$$

Thus the collision integrals $\sigma^2 \Omega^{(l,s)*}$ are a function of reduced temperature $T^* \equiv kT/\epsilon$.

The purpose of presenting Eqs. (5) - (7) is to show the manner in which the potential energy φ influences the transport properties. The potential appears explicitly in the integrand for the angle of deflection and is then averaged by three integrations. Consequently, the collision integrals are insensitive to the details of the intermolecular potential, and we cannot expect experimental transport property measurements to provide much information about the force law. To put it another way, the experimental data cannot be used to determine the

potential; the data can only be used to veto candidate potentials.

For most potential energy functions Eqs. (5) - (7) must be evaluated numerically. The first such calculations for a realistic force law - the Lennard-Jones (12-6) potential - were carried out independently by four different groups[3-6]. Furthermore, the Wisconsin group[5] showed that experimental viscosity data could be fit rather well to yield molecular constants σ and ϵ in reasonable agreement with corresponding parameters obtained from equation of state data.

The Lennard-Jones (12-6) potential

$$\varphi(r) = 4\epsilon \left[\left(\frac{\sigma}{r}\right)^{12} - \left(\frac{\sigma}{r}\right)^{6} \right] \tag{8}$$

combines an inverse sixth power attractive potential with an inverse twelfth power repulsion. The attractive portion has a theoretical basis in the dispersion forces, but the twelfth power repulsion was chosen merely for mathematical convenience. In view of the considerable success of the Lennard-Jones (12-6) potential it is not surprising that the next step was to build some flexibility into the repulsive part of the potential. This was accomplished by introducing an exponential repulsion in place of the inverse twelfth power repulsion; the collision integrals for these potentials, shown in Fig. 1, have been computed by Mason[7,8]. The Lennard-Jones (12-6) potential is also shown in Fig. 1 for purposes of comparison.

The exponential-6 potential serves very well for the noble gases and other molecules that are approximately spherical. Figure 2 shows experimental viscosity data for argon over a wide temperature range; a curve computed for rigid elastic spheres is shown as a dashed line. The potential functions are also shown in Fig. 2. The exponential-6 potential has been chosen[8] to take account of equation of state and crystal properties as well as viscosity coefficients. For

example, the interatomic distance in solid argon is 3.8 Angstroms - just inside of the minimum of the potential energy curve. The same potential also provides a satisfactory explanation of the thermal conductivity (Fig. 3) and self-diffusion coefficient (Fig. 4) for argon.

Since theoretical calculations have been very successful in describing the transport properties for valence-saturated nonpolar gases, it is not surprising that the collision integrals have now been computed for potentials applicable to other situations.

Molecules possessing permanent dipole moments have an intermolecular potential that is not spherically symmetric. The dipoles give rise to a contribution to the potential that depends on the orientation of the dipoles and the inverse cube of the intermolecular separation. An appropriate potential for such molecules is the Stockmayer potential

$$\varphi = 4\epsilon\left[\left(\frac{\sigma}{r}\right)^{12} - \left(\frac{\sigma}{r}\right)^{6} + \delta\left(\frac{\sigma}{r}\right)^{3}\right] \qquad (9)$$

Here δ is a function of the angular orientation of the molecules and also the strength of the dipole moment. It has not as yet been possible to calculate transport properties for this angle-dependent potential. However, collision integrals have been calculated for Stockmayer potentials modified by assuming δ a constant[9]. These potentials are shown in Fig. 5; at the extremes of $\delta = \pm 2.5$ the long-range part of the potential is completely dominated by the inverse cube term. (For comparison the Lennard-Jones (12-6) potential is shown as a dashed curve ($\delta = 0$).)

These collision integrals may be applied to polar gases if it is assumed that the relative orientation of the colliding dipoles remains fixed through the important part of the collision trajectory around the distance of closest

approach. The collision integrals are then averaged over all possible relative orientations[9]. Computed and experimental viscosities of steam (δ = 1.2) are shown in Fig. 6. The fit of the data is not perfect - the experimental data show a temperature dependence that is somewhat steeper that the theoretical prediction - but it is an improvement over the fit obtained by using a simple Lennard-Jones (12-6) potential.

Collision integrals have also been computed for the range of Morse potentials shown in Fig. 7[10]. The potentials with the very broad wells can be applied to interactions between atoms corresponding to chemically bound molecules (for example, the $^1\Sigma$ interaction between two hydrogen atoms, which corresponds to the hydrogen molecule). The potentials with the narrow wells have been used to fit data on nonpolar, valence-saturated molecules.

Collision integrals also have been computed for a number of other potentials including the repulsive exponential potential[11] (for molecules at high temperatures, as well as nonbonding interactions between atoms or free radicals), the shielded coulombic potential[12] (for repulsive interactions in ionized gases), several (12-6-4) potentials[13] (for ion-neutral interactions), several inverse power attractive and repulsive potentials[14], and also estimates for the attractive exponential[15] (for low-temperature interactions between atoms or free radicals corresponding to bound molecular states).

Thus the collision integrals are now available for a wide variety of potentials. Hence, if the details of a potential energy curve are known, a good match to it can be selected from the "library" of calculations already at hand.

HEAT CONDUCTION IN CHEMICALLY REACTING GASES

At high temperatures many gases are partially dissociated and undergo a variety of chemical reactions. In reacting gases, heat transport may be considerably larger than in "frozen" (nonreacting) mixtures. Large amounts of heat can be carried as chemical enthalpy of molecules that diffuse because of concentration gradients. These gradients exist, in turn, because the gas composition varies with temperature. For example, in a gas that absorbs heat by dissociating as the temperature is raised, heat is transported when a molecule dissociates in the high-temperature region and the fragments diffuse toward the cooler region. In the low-temperature region the fragments recombine and release the heat absorbed at high temperature.

When chemical reaction rates are very high, chemical equilibrium can be assumed to exist locally throughout a gas mixture. It is then possible, by differentiating the equilibrium relationships, to relate the concentration gradients to the temperature gradient. In this event one can define an equilibrium thermal conductivity λ_e independent of apparatus geometry:

$$\lambda_e = \lambda_f + \lambda_r \tag{10}$$

where λ_f is the conductivity in the absence of reaction (the "frozen" thermal conductivity) and λ_r is the augmentation due to the reactions.

A general expression for the thermal conductivity due to chemical reactions has been developed[16,17] that is applicable to mixtures involving any number of reactants, inert diluents, and chemical equilibria, provided chemical equilibrium exists locally in the temperature gradient. For a simple dissociation of the type $A \rightleftarrows nB$ the thermal conductivity due to chemical reaction is

$$\lambda_r = \frac{D_{AB}}{RT} \frac{\Delta H^2}{RT^2} \frac{x_A x_B}{(nx_A + x_B)^2} \tag{11}$$

Here D_{AB} is the binary diffusion coefficient between components A and B, ΔH is the heat of reaction, and x_A, x_B are the mole fractions of the components. Note that unless both species are present, λ_r is zero. Furthermore, since in a dissociating gas the gas composition varies with pressure, we expect the heat conductivity to vary with pressure also. This is in contrast to the behavior of nonreacting gases, for which the heat conductivity is independent of pressure.

Experimental and theoretical conductivities for the $N_2O_4 \rightleftarrows 2NO_2$ system at one atmosphere are shown in Fig. 8[18]. The dashed curve indicates the frozen conductivity. Thus λ_r is the major contribution to the heat conductivity; at the maximum (where the mass fractions of N_2O_4 and NO_2 are equal) the conductivity is comparable to that of a light gas such as helium.

The theoretical expression for a system involving two reactions has been tested[19] for the case of hydrogen fluoride vapor. At moderate pressures the PVT behavior of hydrogen fluoride can be described in terms of a monomer-hexamer equilibrium, while low pressure data suggest a dimer as well. Although the actual state of the vapor is uncertain, it appears that at low and moderate pressures the equilibria

$$2HF \rightleftarrows (HF)_2 \qquad \Delta H_2 = 7.4 \text{ kcal}$$

$$6HF \rightleftarrows (HF)_6 \qquad \Delta H_6 = 40.5 \text{ kcal}$$

serve to specify the system rather well.

Computed and experimental[20] thermal conductivities are compared in Fig. 9. The solid line was computed assuming both dimer and hexamer equilibria, whereas the dashed line was computed considering only the hexamer equilibrium. Note the extreme pressure dependence of the thermal conductivity. The maximum conductivity is more than three times that of hydrogen at the same temperature and some 33

times the frozen thermal conductivity expected in the absence of reaction. The inclusion of a dimer equilibrium markedly improves the agreement between theory and experiment in the low-pressure region.

The experimental studies on nitrogen tetroxide and hydrogen fluoride prove the validity of the theoretical expressions for thermal conductivity of reacting gases in chemical equilibrium. Recently the theory has been successfully applied to data for the $PCl_5 \rightleftarrows PCl_3 + Cl_2$ equilibrium[21].

Thus far we have considered systems where the chemical reactions are so rapid that chemical equilibrium prevails locally at all points in the gas mixture. Let us now consider the reduction of heat transport caused by reduced reaction rates. A general expression has been derived[22] for the apparent "thermal conductivity" of reacting mixtures in which a single reaction proceeds at a finite rate. In contrast to systems where reaction rates are either very high or very low, it is found that heat conduction depends on the geometry and scale of the system and also the catalytic activity of the surfaces.

For a plane parallel plate geometry, with one surface noncatalytic and the other surface a perfect catalyst, the effective "thermal conductivity" is

$$\lambda^* = \frac{\lambda_e \lambda_f}{\lambda_f + \lambda_r \dfrac{\tanh \varphi}{\varphi}} \tag{12}$$

where

$$\varphi^2 \equiv \frac{\lambda_e}{\lambda_f \lambda_r} \frac{\Delta H^2}{RT^2} \mathcal{R} l^2$$

Here $\mathcal{R}$ is the chemical reaction rate at equilibrium (that is the total rate in either direction - not the net rate, which is zero, of course), and l is the distance between the plates. For simple systems it can be shown that

$$\varphi^2 = \frac{\lambda_e}{\lambda_f} \frac{\tau_{Diff}}{\tau_{chem}} \tag{13}$$

If the diffusion time τ_{Diff} is short in comparison with the chemical relaxation time τ_{chem}, $\varphi \to 0$, $\tanh \varphi/\varphi \to 1$, and $\lambda^* \to \lambda_f$. In other words, the concentration gradients are washed out by diffusion and the frozen conductivity is obtained. On the other hand if the chemical time is short, the concentration gradients are maintained, $\varphi \to 1$, $\tanh \varphi/\varphi \to 0$, and $\lambda^* \to \lambda_e$.

The theory has been applied to the low-pressure measurements[18] on the $N_2O_4 \rightleftarrows 2NO_2$ system, as shown in Fig. 10. The upper and lower dashed curves are respectively, the computed equilibrium and frozen conductivities. The remaining two curves are calculations of λ^* for various reaction rates, assuming negligible chemical reaction on the surfaces. Near atmospheric pressure the experimental data lie on the equilibrium conductivity curve, which is in agreement with Fig. 8.

At low pressures the dissociation of N_2O_4 is a fast bimolecular reaction:

$$N_2O_4 + M \to 2NO_2 + M$$

The curve marked $M = N_2$ has been calculated by using the rate data of Carrington and Davidson[23] for the dissociation of N_2O_4 in nitrogen. The solid curve has been calculated by assuming the second order rate is sevenfold greater when undiluted N_2O_4 - NO_2 mixtures dissociate; this is in conformity with the experiments of Bauer and Gustavson[24]. The agreement between theory and experiment is very satisfactory.

THERMAL CONDUCTIVITY OF POLYATOMIC GASES

It is convenient to discuss the thermal conductivity of a polyatomic gas in terms of its relationship to the viscosity through the dimensionless ratio

$$f = \lambda M/\eta C_v \qquad (14)$$

Here M is the molecular weight and C_v is the constant volume molar heat capacity. According to ultrasimplified kinetic theory, $f = 1$; however, the

rigorous Chapman-Enskog theory for monatomic gases predicts that f should be very nearly 5/2. This is due to the fact that translational energy is a function of molecular velocity; the molecules possessing the most energy are the most rapid, have the longest mean free paths, and hence make an enhanced contribution to the heat transport. Indeed, experiment confirms that f is about 2.5 for the noble gases. This is illustrated in Fig. 11 where data for argon are shown over a temperature from about 100° to 300° K. The data points represent measurements[25] that provides a direct determination of f.*

For polyatomic gases, f is less than 2.5 and tends to be smallest when the molar heat capacity is largest and originates mostly from the internal energy modes. Consequently, Eucken[27] suggested that the transport of translation and internal energy be considered separately, and proposed

$$fC_v = f_{trans} C_{v,trans} + f_{int} C_{int} \qquad (15)$$

($C_{v,trans}$ and C_{int} are the translational and internal contributions to the total heat capacity C_v.) Eucken assumed $f_{trans} = 5/2$, by analogy with the monatomic gases. However, because there is little correlation between molecular velocity and <u>internal</u> energy, Eucken assumed $f_{int} = 1$ (the result of the ultra-simple theory that neglects the velocity-translational energy correlation).

Ubbelohde[28] pointed out that molecules with excited internal energy states may be regarded as different chemical species and that the flow of internal energy can be considered as energy transport due to diffusion of the excited states. This concept leads to the result $f_{int} = \rho D/\eta$, so that

---

*The method involves measurement of the adiabatic recovery temperature T_r attained on a flat plate in a high-velocity subsonic gas stream. The recovery temperature is related to the stream temperature T_s and total temperature T_t through the recovery factor $r \equiv (T_r-T_s)/(T_t-T_s)$. To a very good approximation $f = \gamma/r^2$ where γ is the specific heat ratio.

$$f_{ME} C_v = \frac{15}{4} R + \frac{\rho D}{\eta} C_{int} \qquad (16)$$

For many realistic force laws $\rho D/\eta \approx 1.3$ over a large temperature range. To justify this modified Eucken approximation [Eq. (16)] it is tacitly assumed that inelastic collisions are rare. This is necessary in order that the translational velocity distribution function should not be unduly perturbed, so that the translational conductivity can be related to the viscosity as in the case of the noble gases. On the other hand, there must be enough inelastic collisions to maintain the internal energy states in equilibrium with the local temperature.

Mason and Monchick[29] have recently derived explicit expressions for f_{trans} and f_{int} from the formal kinetic theory of polyatomic gases. By systematically including terms involving inelastic collisions they obtained the modified Eucken expression as a first approximation, and, as a second approximation, an expression dependent on the relaxation times for the various internal degrees of freedom. For nonpolar gases their result may be written

$$f_{MM} C_v = \frac{15}{4} R + \frac{\rho D}{\eta} C_{int} - \frac{2}{\pi}\left(\frac{5}{2} - \frac{\rho D}{\eta}\right)^2 \frac{C_{rot}}{Z_{rot}} \qquad (17)$$

Here C_{rot} is the rotational contribution to the heat capacity (R for linear molecules, $\frac{3}{2} R$ for nonlinear molecules) and Z_{rot} is a collision number for rotational relaxation:

$$Z_{rot} = \tau_{rot}/\tau_{coll} = \frac{4}{\pi} \frac{P\tau_{rot}}{\eta} \qquad (18)$$

where τ_{rot} is the rotational relaxation time and $\tau_{coll} = (\pi/4)(\eta/P)$ is the mean time between collisions.

Experimental f values for nitrogen[25], carbon dioxide[30,31], and hydrogen[25] are shown in Figs. 12, 13, and 14. The upper dashed curves correspond to the modified Eucken approximation [Eq. (16)], while the solid lines have been

calculated from Mason and Monchick's expression [Eq. (17)] by assuming the temperature-independent collision numbers shown in the figures. The Eucken approximations ($f_{trans} = 2.5$, $f_{int} = 1$) are shown as well for completeness. The data on nitrogen and carbon dioxide lie midway between the Eucken and modified Eucken approximations. In contrast, the hydrogen data scatter about the modified Eucken approximation ($Z = \infty$). Indeed, the hydrogen molecule is unique in that exchange between translational and rotational energy is not easy; collision numbers of a few hundred are predicted from theory and observed experimentally.

Collision numbers determined from f, or recovery factor, are compared with other measurements in Table I. The values from f are generally in accord with those obtained by the other techniques, within the admittedly rather large uncertainties associated with such determinations. The only serious disagreement is in the case of carbon dioxide, where acoustical measurements indicate that 16 collisions are required for relaxation. It seems likely that the acoustic result is in error; it is difficult to see any theoretical reason why carbon dioxide should relax so slowly.

A classical theory for the rotational relaxation of molecules with attractive intermolecular forces (rough spheres and spherocylinders surrounded by square wells) has recently been developed by Sather and Dahler[32]. In the case of rough spheres the rotational relaxation time is

$$\tau_{rot}^{-1} = \frac{16}{3} n\sigma^2 \frac{(4I/m\sigma^2)}{[1 + (4I/m\sigma^2)]^2} \left(\frac{\pi kT}{m}\right)^{\frac{1}{2}} g(\sigma) \qquad (19)$$

Here n is the number of molecules per cm^3, I is the moment of inertia, m is the mass, σ is the diameter of the rough sphere core, while $g(\sigma)$ is the value of the radial distribution function at σ. In the low-density limit,

$g(\sigma) = \exp(\epsilon/kT)$, where ϵ is the depth of the well at σ.

Equation (19) possesses two noteworthy features. First, since the quantity $4I/m\sigma^2$ is generally less than 0.2, the relaxation time depends only weakly on σ, the position of the repulsive core. Secondly, since there is no rotational energy transfer accompanying the velocity impulse at the outer edge of the potential well, the only contribution to the rotational relaxation stems from the impulse at the core. Consequently, the width of the well is unimportant; in fact, Eq. (19) should apply to a Sutherland potential with a rough core - that is, a potential with an inverse sixth power attractive portion to account for Van der Waals forces. We might hope that this model would be suitable for molecules that are approximately spherical.

After combining Eqs. (1), (18), and (19) we find

$$Z_{rot}^{-1} \simeq \frac{5\pi}{12}\left(\frac{4I}{m\sigma^2\Omega(2,2)^*}\right)\exp(\epsilon/kT) \qquad (20)$$

(The term $4I/m\sigma^2$ in the denominator of Eq. (19) has been neglected.) Some experimental results are compared with predictions of Eq. (20) in Table II. Methane, carbon tetrafluoride, and sulfur hexafluoride are approximately spherical, as shown in Fig. 15; for these molecules the agreement between theory and experiment seems very good indeed. The mass distribution parameter $4I/m\sigma^2\Omega(2,2)^*$ varies more than threefold between methane and carbon tetrafluoride; thus the large collision number of methane is probably a direct consequence of the molecule's small moment of inertia. Note that the effect of attractive forces [$\exp(\epsilon/kT)$] is appreciable and roughly doubles the transition probabilities.

The calculations for ethylene and ethane were carried out using average moments of inertia. The Z_{rot}^{-1} values calculated for ethane are in close accord

with experiment, but in the case of ethylene the agreement is not so good. From Fig. 15 it is apparent that the ethane molecule is approximately spherical, whereas the ethylene structure is definitely less compact and symmetric.

It appears, then, that the classical kinetic theory for a rough spherical molecule with attractive forces may provide a lower limit to the collision probability for rotational relaxation, Z_{rot}^{-1}, for nonlinear molecules. Molecules such as CH_4, CF_4, SF_6, and C_2H_6 are reasonably represented by this model, whereas less symmetric molecules such as C_2H_4 have large transition probabilities, or shorter relaxation times. As a matter of fact the theory of Brout[31,33] for the relaxation of diatomic molecules such as nitrogen and oxygen also indicates that the deviation of the intermolecular potential from spherical symmetry is an important parameter.

Thus we conclude that Mason and Monchick's approximate theory for the heat conductivity of polyatomic gases is at least qualitatively correct. Furthermore, the following factors seem of profound importance in determining rotational relaxation times for nonpolar gases:

(1) The mass distribution (characterized by $4I/m\sigma^2$)

(2) The strength of the intermolecular attractive forces (characterized by ϵ/kT)

(3) The deviation of the molecular force field from spherical symmetry

CONCLUDING REMARKS

In the past decade there have been substantial advances in methods for calculating the transport properties of gases and gas mixtures. Collision integrals have been calculated for a considerable variety of realistic potential energy functions. The effects of chemical reaction and chemical rate phenomena

seem to be well understood, and there is gratifying accord between theory and experiment. Finally, the theory of Mason and Monchick[29] shows great promise as a description of the behavior of polyatomic gases.

What remains for the future? First, it is to be hoped that the relaxation theory of Mason and Monchick will be extended to gas mixtures, and that there will be further testing of the theory, both for pure gases and gas mixtures. There is room for more work on the heat conductivity of polar gases. The conductivities of highly polar gases seem anomalously low in relation to their viscosity (in other words, f values are small), and it has been suggested[29] that this effect is largely due to a resonant exchange of rotational quanta, presumed probable on grazing self-collisions of polar molecules. However, results of experiments designed to test this notion[34] have been somewhat ambiguous. Finally, theoretical studies on the kinetic theory of nonspherical molecules should be encouraged.

REFERENCES

1. J. O. Hirschfelder, C. F. Curtiss, and R. B. Bird, Molecular Theory of Gases and Liquids, Wiley, New York (1954).

2. Reference 1, p. 527.

3. T. Kihara and M. Kotani, Proc. Phys. Math. Soc. Japan 24, 76 (1942).

4. J. de Boer and J. Van Krankendonk, Physica 14, 442 (1948).

5. J. O. Hirschfelder, R. B. Bird, and E. L. Spotz, J. Chem. Phys. 16, 968 (1948).

6. J. S. Rowlinson, J. Chem. Phys. 17, 101 (1949).

7. E. A. Mason, J. Chem. Phys. 22, 169 (1954).

8. E. A. Mason, and W. E. Rice, J. Chem. Phys. 22, 843 (1954).

9. L. Monchick and E. A. Mason, J. Chem. Phys. 35, 1676 (1961).

10. S. E. Lovell and J. O. Hirschfelder, Theoretical Chemistry Laboratory, University of Wisconsin Rept. WIS-AF-21, (June 1962); also private communication from S. E. Lovell.

11. L. Monchick, Phys. Fluids 2, 695 (1959).

12. R. L. Liboff, Phys. Fluids 2, 40 (1959).

13. E. A. Mason and H. W. Schamp, Jr., Ann. Phys., New York 4, 233 (1958).

14. T. Kihara, M. H. Taylor, and J. O. Hirschfelder, Phys. Fluids 3, 715 (1960).

15. R. S. Brokaw, Phys. Fluids 4, 944 (1961).

16. J. N. Butler and R. S. Brokaw, J. Chem. Phys. 26, 1636 (1957).

17. R. S. Brokaw, J. Chem. Phys. 32, 1005 (1960).

18. K. P. Coffin and C. O'Neal, Jr., NACA TN 4209 (1958).

19. R. S. Brokaw, Planetary Space Sci. 3, 238 (1961).

20. E. U. Franck and W. Spalthoff, Naturwiss, 40, 580 (1953).

21. P. K. Chakraborti, J. Chem. Phys. 38, 575 (1963).

22. R. S. Brokaw, J. Chem. Phys. 35, 1569 (1961).

23. T. Carrington and N. Davidson, J. Phys. Chem. 57, 418 (1953).

24. S. H. Bauer and M. R. Gustavson, Discussions Faraday Soc. 17, 69 (1954).

25. C. O'Neal, Jr. and R. S. Brokaw, Phys. Fluids 5, 567 (1962).

26. E. R. G. Eckert and T. F. Irvine, Jr., J. Appl. Mech. 24, 25 (1957).

27. A. Eucken, Physik Z. 14, 324 (1913).

28. A. R. Ubbelohde, J. Chem. Phys. 3, 219 (1935).

29. E. A. Mason and L. Monchick, J. Chem. Phys. 36, 1622 (1962).

30. J. L. Novotny and T. F. Irvine, Jr., J. Heat Transfer 83, 125 (1961).

31. C. O'Neal, Jr., and R. S. Brokaw, Phys. Fluids 6, 1675 (1963).

32. N. F. Sather and J. S. Dahler, J. Chem. Phys. 37, 1947 (1962).

33. R. Brout, J. Chem. Phys. 22, 1189 (1954).

34. C. E. Baker and R. S. Brokaw, J. Chem. Phys. 40, 1523 (1964).

TABLE I. - COMPARISON OF COLLISION NUMBERS FOR ROTATIONAL RELAXATION[31]

Gas	f (determined from recovery factor)	Acoustical	Low-pressure thermal conductivity	Shock thickness	Impact tube
N_2	7	5.3, 6, 4-6		5.5	<7, <14
O_2	12	2-4, 4.1, 12, 14, 12-30	20	7	
H_2	Large	240-360	300	>150	160, 310
CO_2	2.4	16			
CH_4	9	14-17			

TABLE II. - EXPERIMENTAL DATA FOR SOME NONLINEAR MOLECULES COMPARED WITH ROUGH SPHERE THEORY

	Methane	Carbon tetrafluoride	Sulfur hexafluoride	Ethane	Ethylene
$4I/m\sigma^2\Omega(2,2)^*$	0.05	0.16	0.14	0.09	0.08
$\exp(\epsilon/kT)$	1.7	1.6	2.1	2.1	2.2
Z^{-1} calc	.11	.33	.38	.25	.23
Z^{-1} expt	.11	.33	.36	.25	.42
Z expt	9	3.0	2.8	4	2.4

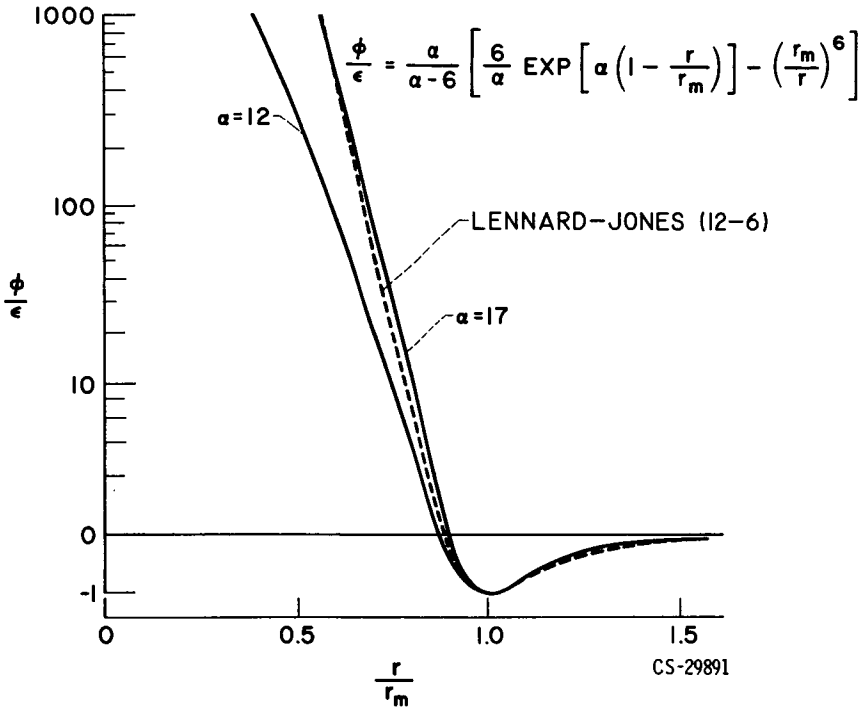

Fig. 1. - Exponential - 6 potentials for which collision integrals have been computed.

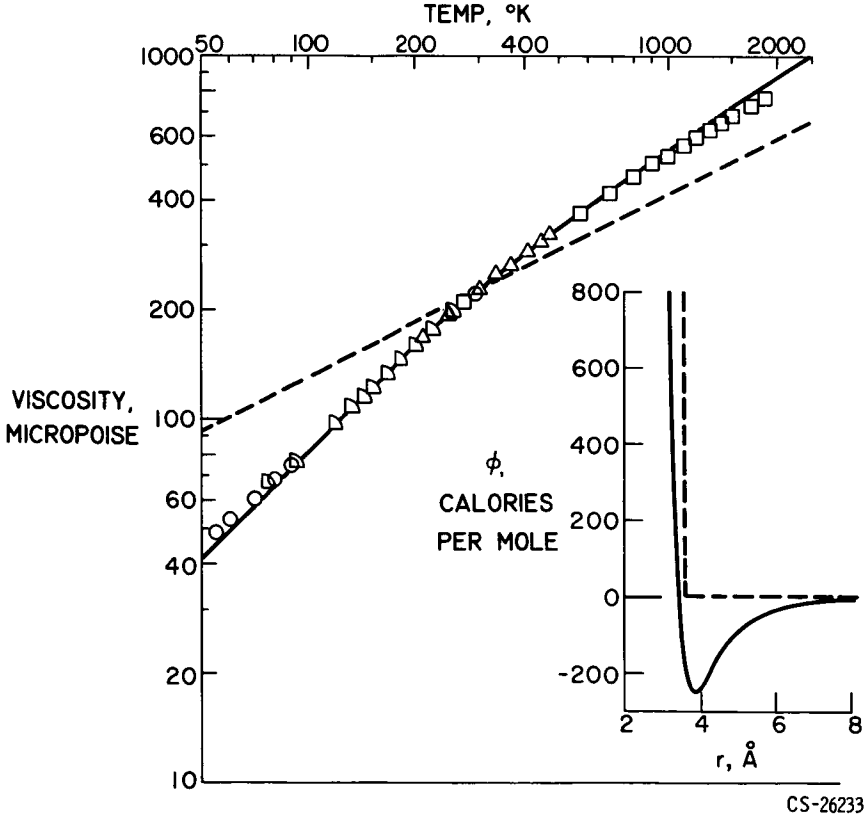

Fig. 2. - Viscosity of argon.

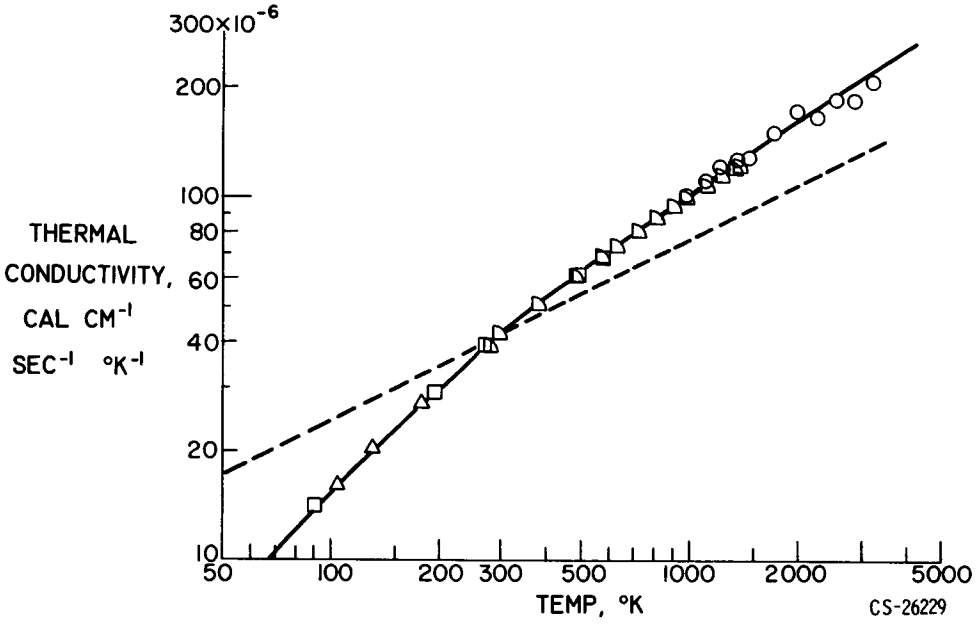

Fig. 3. - Thermal conductivity of argon.

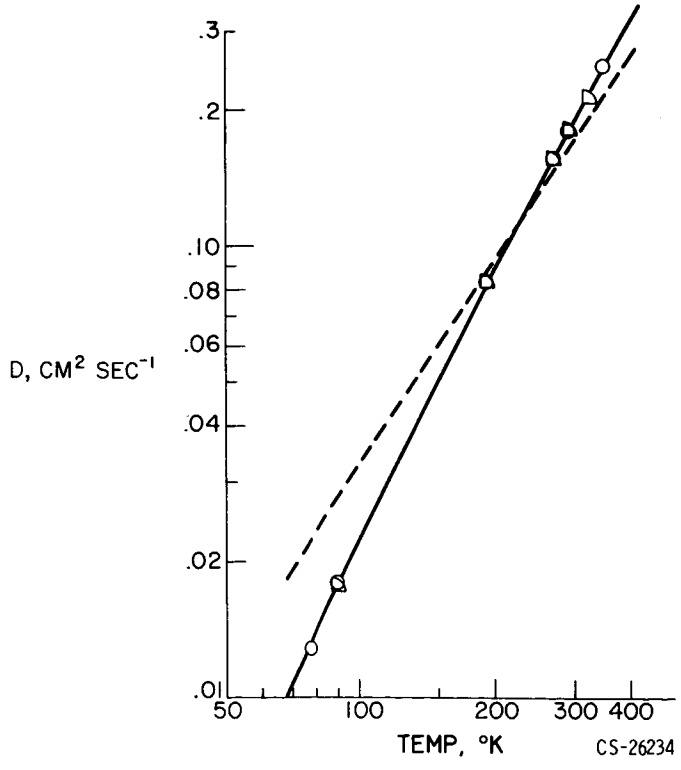

Fig. 4. - Self-diffusion coefficient of argon.

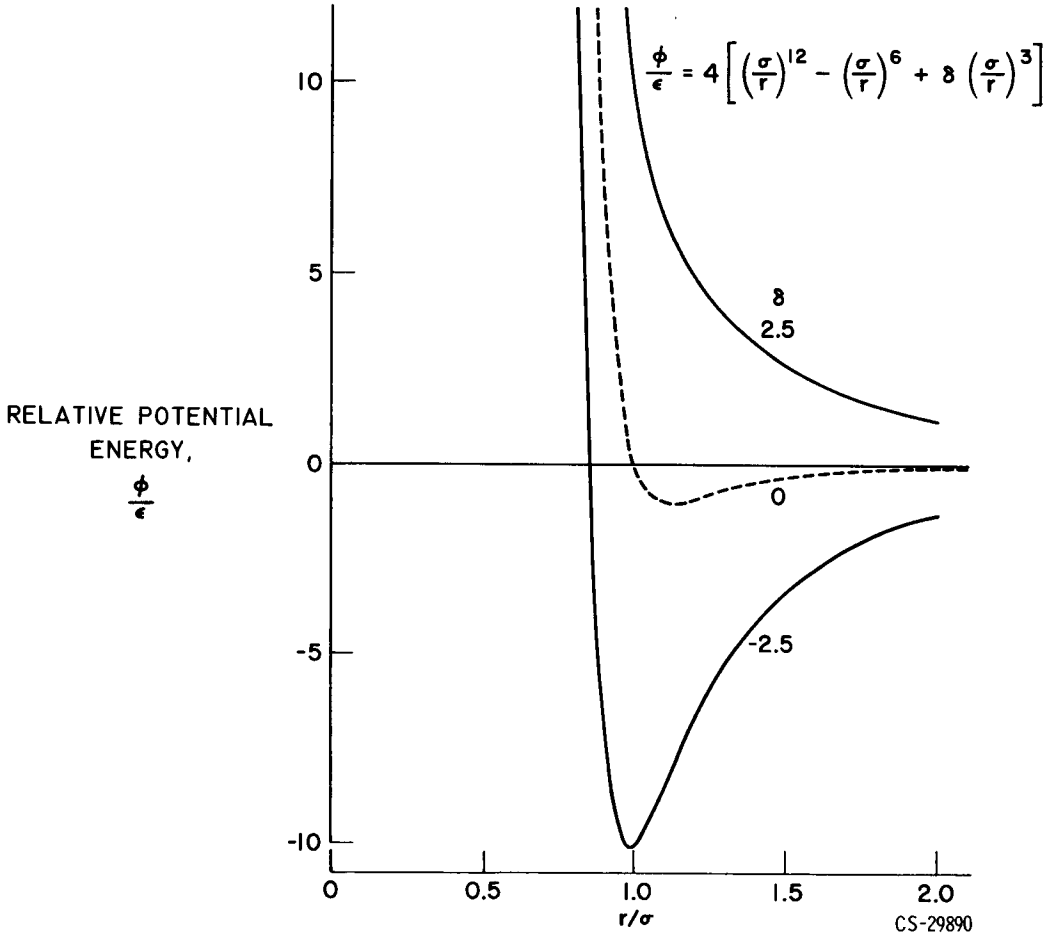

Fig. 5. - Modified Stockmayer potentials for which collision integrals have been computed.

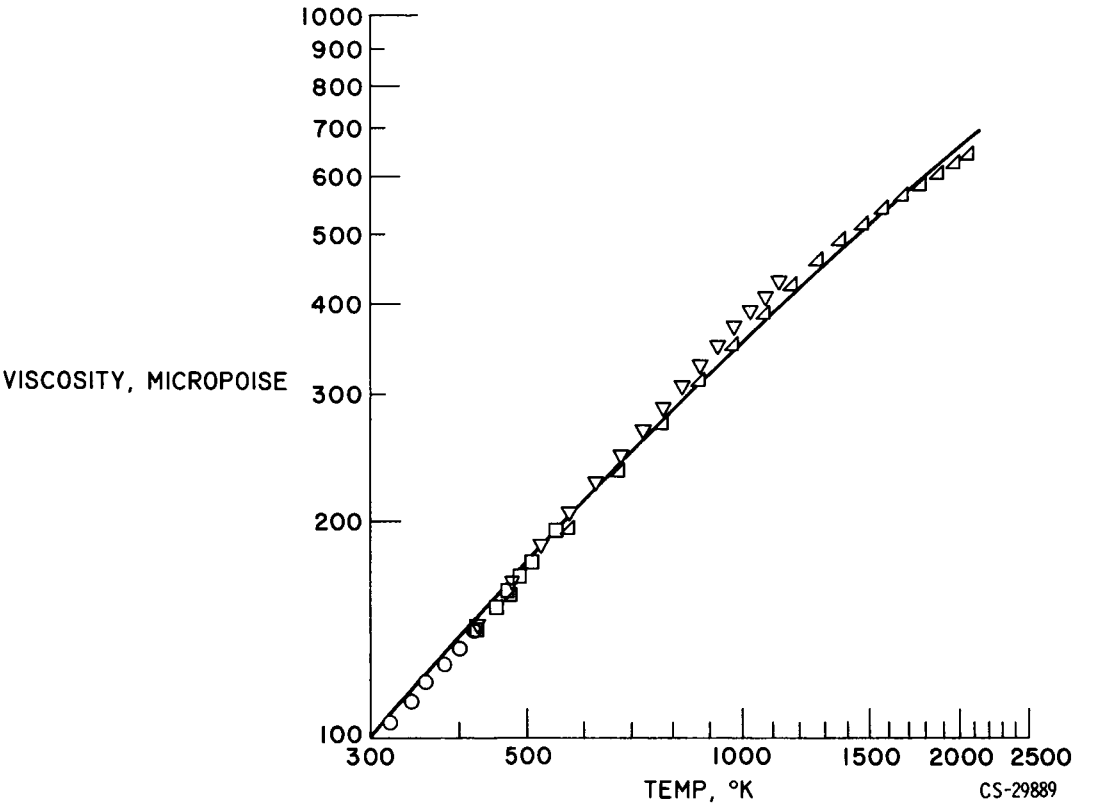

Fig. 6. - Viscosity of water vapor.

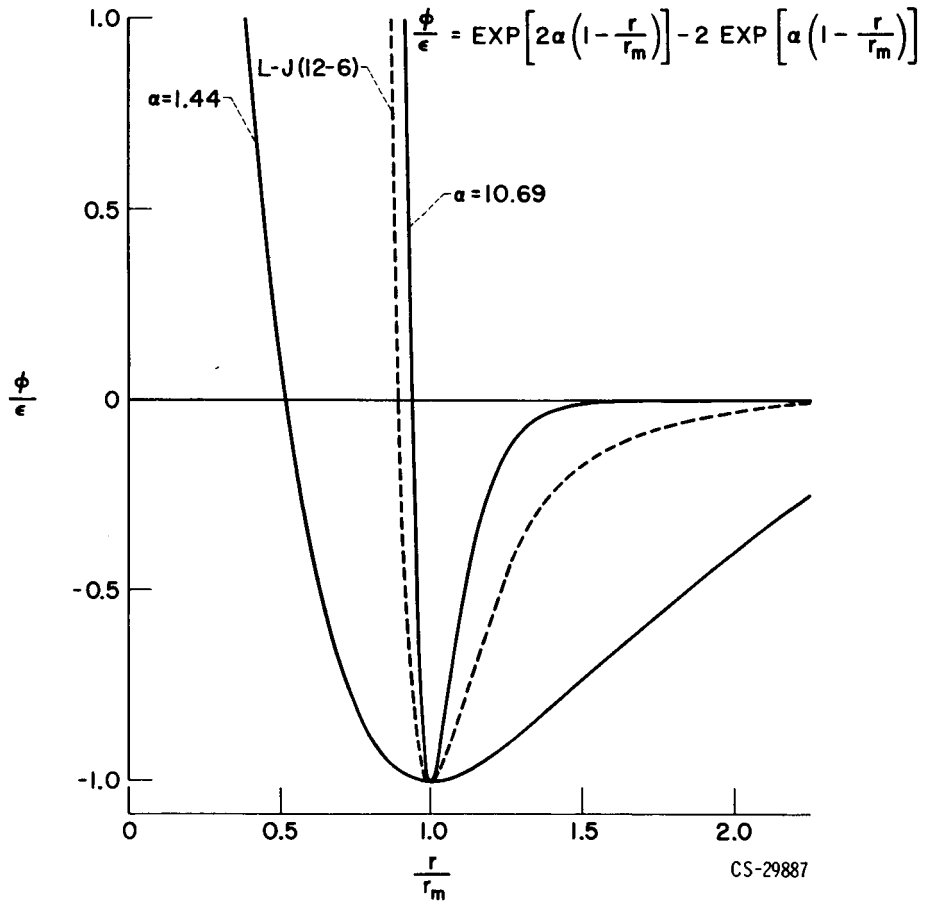

Fig. 7. - Morse potentials for which collision integrals have been computed.

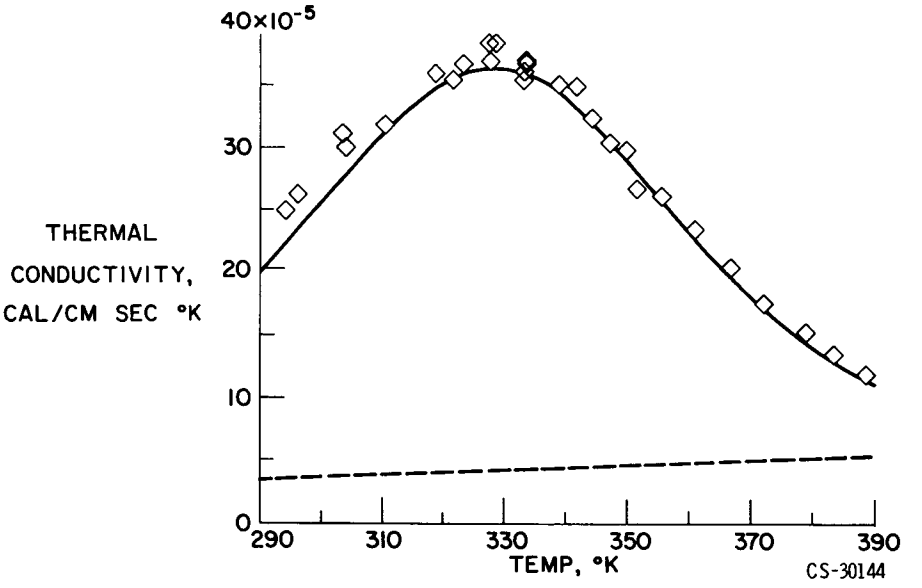

Fig. 8. - Thermal conductivity of the N_2O_4 -NO_2 system at atmospheric pressure.

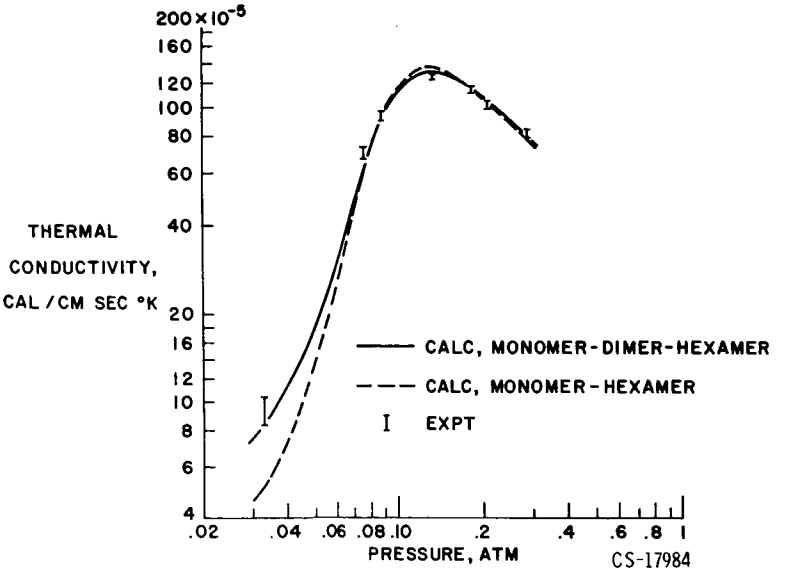

Fig. 9. - Thermal conductivity of hydrogen fluoride vapor at 267.7° K.

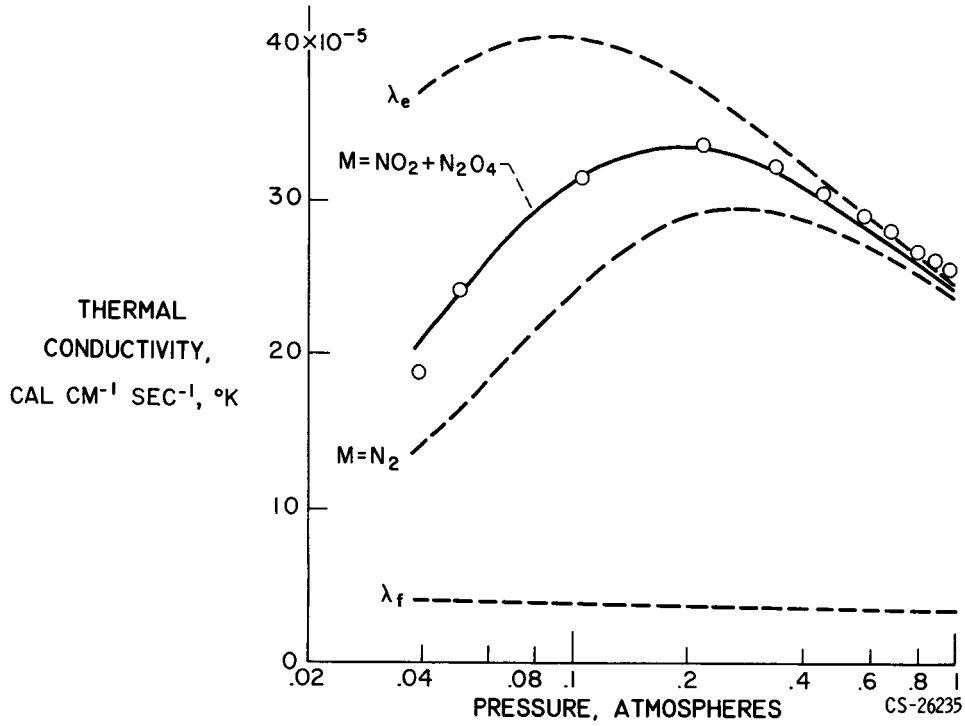

Fig. 10. - Thermal conductivity of the $N_2O_4 \rightleftarrows 2NO_2$ system at 296° K.

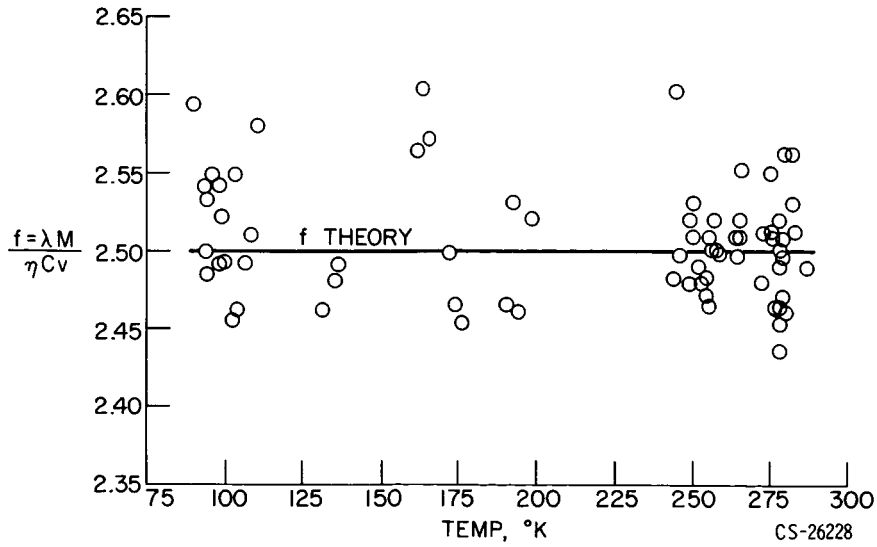

Fig. 11. - Experimental and theoretical values of f for argon.

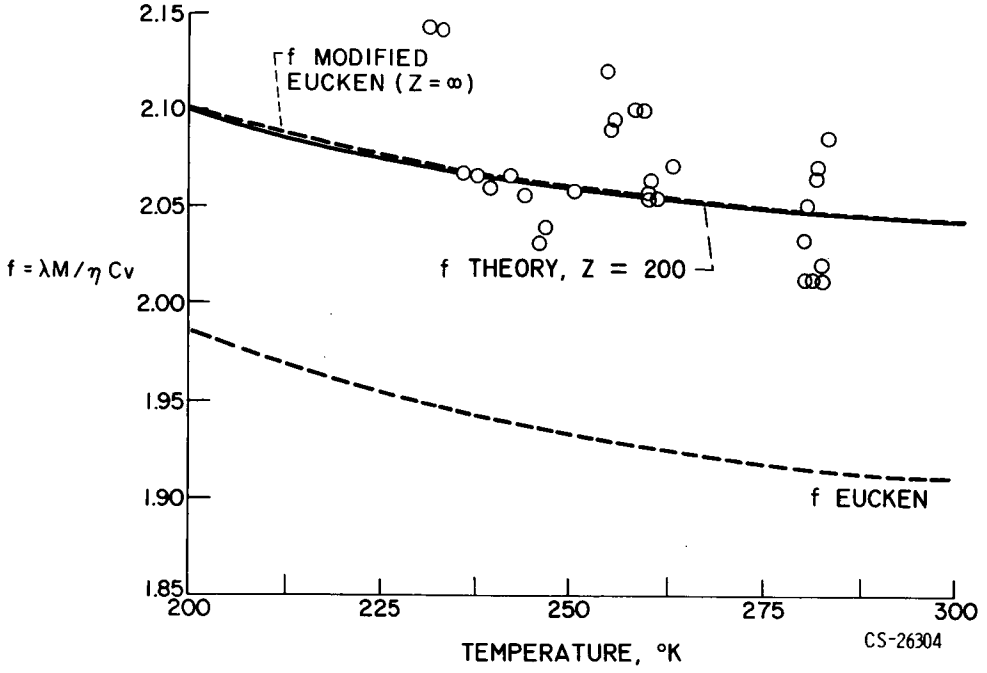

Fig. 14. - Experimental and theoretical values of f for hydrogen.

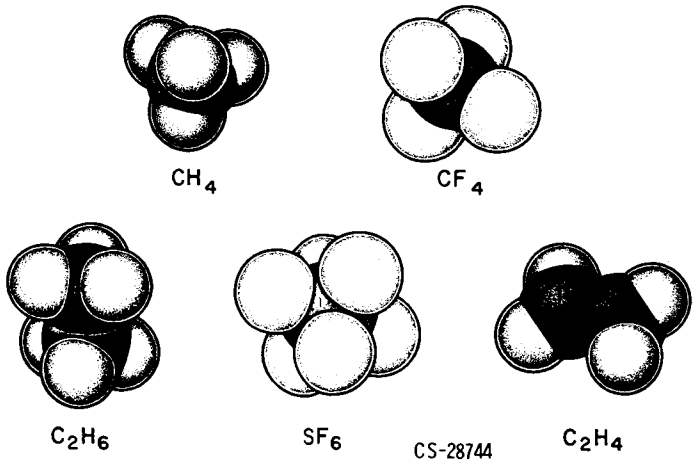

Fig. 15. - Configurations of nonlinear molecules.